

# Detection of Kinase Activity Using Versatile Fluorescence Quencher Probes\*\*

Hyun-Woo Rhee, Seung Hwan Lee, Ik-Soo Shin, So Jung Choi, Hun Hee Park, Kyungja Han, Tai Hyun Park,\* and Jong-In Hong\*

Protein phosphorylation is the most universal form of posttranslational modification of cell-signal transduction in living organisms. The human kinome<sup>[1a]</sup> comprises 518 protein kinases that control protein phosphorylation; irregular control of protein phosphorylation is a major cause of diseases such as cancer.<sup>[1b]</sup> Therefore, accurate probing of the kinase activity of a target protein is crucial for cancer diagnosis and high-throughput screening of anticancer drugs.<sup>[2,3]</sup>

For the high-throughput analysis of kinase activity, several research groups have developed various types of protein or peptide chips using radioactive labeling<sup>[2a]</sup> with [<sup>32</sup>P<sub>γ</sub>]-adenosine 5'-triphosphate (ATP) or using antibody hybridization.<sup>[2b]</sup> However, a crucial problem involved in the use of these on-chip detection methods<sup>[2]</sup> is that some kinases show decreased activities on the surfaces of chips because of reduced enzyme accessibility to the substrate.<sup>[2d]</sup>

In recent years, several pharmaceutical and biotechnology companies have developed homogeneous kinase assay systems based on fluorescence polarization (FP) for developing anticancer drugs.<sup>[3]</sup> These platforms (kinase assay systems) utilize peptide substrates with an N-terminal fluorophore and phospho-specific antibodies<sup>[3b]</sup> or phosphopeptide (or phosphoprotein)-binding nanoparticles (IMAP).<sup>[3c]</sup> However, FP-based detection has been reported to be very sensitive to fluorescence interference, and it is liable to produce false positives when used to screen a large number of compounds.<sup>[3d]</sup> Furthermore, there are no reports on the real-time monitoring of kinase activity in cell lysates through FP-based kinase detection; this is because many cellular components can bind to the fluorescent peptides and produce false positives for FP.

Recently, peptide- or protein-linked synthetic fluorescent probes that are sensitive to certain protein kinases have been reported by the research groups of Lawrence, Imperiali, Sames, and Hamachi.<sup>[4-7]</sup> Ting, Tsien, and co-workers used fluorescent proteins to develop an *in vivo* probe system to detect kinase.<sup>[8]</sup> These synthetic probes enabled real-time fluorescence monitoring of the specific activity of kinases in cellular lysates, and exhibited immense potential for use in the development of kinase activity inhibitors for certain kinases.

However, it is still difficult to predict and determine the optimal sites for attaching fluorophores near the phosphorylated sites on the substrate peptides or proteins; the attachment of these fluorophores is necessary to induce significant changes in the fluorescence signal after phosphorylation of the substrate peptides or proteins by a specific kinase. Therefore, a general strategy for developing a synthetic fluorescent kinase probe is desired.

We designed chemosensors Dab-DPA and PTZ-DPA (Scheme 1) to develop a simple but powerful kinase assay tool based on fluorescence intensity changes (ON/OFF). Using these chemosensors, we show for the first time the diagnosis of chronic myelogenous leukemia (CML) through real-time fluorescence monitoring of Abelson (Abl) tyrosine kinase activity and the development of a fluorescence-based homogeneous kinase assay system on a microfluidic chip.

As shown in Scheme 1, Dab-DPA consists of a bis(Zn<sup>2+</sup>-dipicolylamine) complex and a dabicyl (Dab) fluorescence quencher, and PTZ-DPA consists of the dipicolylamine complex and a phenothiazine (PTZ) fluorescence quencher. Dab and PTZ quench fluorescence by Förster resonance energy transfer (FRET)<sup>[9]</sup> and photoinduced electron transfer (PET),<sup>[10,11g]</sup> respectively. The bis(Zn<sup>2+</sup>-dipicolylamine) complex is a well-known synthetic receptor that strongly and selectively binds to phosphate in aqueous solution.<sup>[11]</sup> Dab-DPA and PTZ-DPA are synthesized in a few steps (see the Supporting Information).

PTZ is a good fluorescence quencher but there are very few reports on its use as such, except for the isoalloxazine ring of flavins.<sup>[10,11g]</sup> To prove that PTZ can be used as a general fluorescence quencher for other fluorophores, such as carboxyfluorescein (FAM) or tetramethylrhodamine (TMR), we performed electrochemical analyses of PTZ, FAM, and TMR.

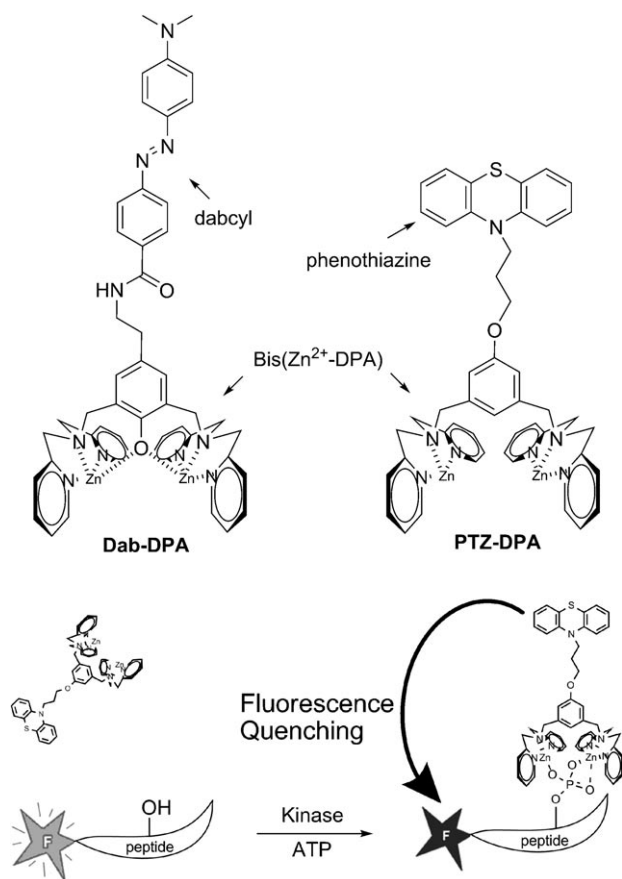
Figure 1a shows the cyclic voltammograms of 1 mM PTZ, TMR, and FAM; the Pt-disk working electrode is immersed in acetonitrile with 0.1 M tetrabutylammonium hexafluorophosphate (TBAPF<sub>6</sub>) as supporting electrolyte. The observed waves are assigned to the oxidation of PTZ and the fluorophores (TMR and FAM). PTZ undergoes nearly Nernstian oxidation at  $E_{1/2,ox} = 0.63$  V with a peak separation

[\*] Dr. H.-W. Rhee, S. H. Lee, Dr. I.-S. Shin, S. J. Choi, Prof. Dr. T. H. Park, Prof. Dr. J.-I. Hong  
Department of Chemistry  
School of Chemical & Biological Engineering  
Seoul National University, Seoul 151-747 (Korea)  
Fax: (+82) 2-889-1568  
E-mail: thpark@snu.ac.kr  
jihong@snu.ac.kr

Dr. H. H. Park, Prof. Dr. K. Han  
Department of Clinical Pathology  
Catholic University Medical College, Seoul (Korea)

[\*\*] This study was supported by a National Research Foundation (NRF) grant funded by the MEST (Grant Nos. 2009-0080734, 2009-0081997, 2010-0000825, WCU project R32-2009-000-10213-0). H.-W.R. is the recipient of POSCO T.J. Park postdoctoral fellowship. Gleevec was provided by Novartis.

Supporting information for this article is available on the WWW under <http://dx.doi.org/10.1002/anie.201000879>.



**Scheme 1.** Top: Chemical structures of Dab-DPA and PTZ-DPA.

Bottom: Detection of protein kinase activity based on fluorescence intensity (ON/OFF) using PTZ-DPA. Dab = dabcyl, DPA = bis( $Zn^{2+}$ -dipicolylamine) complex, PTZ = phenothiazine.

of 71 mV. The peak current ratio is approximately unity ( $i_{pc}/i_{pa}=0.97$ ) at a scan rate of  $200 \text{ mV s}^{-1}$ ; this suggests that the oxidation results in a stable radical cation. However, the cyclic voltammograms recorded during the oxidation of TMR show successive irreversible oxidation waves in the range of 0.87–1.96 V under the same conditions as for the oxidation of PTZ. Therefore, the half-wave potential of the first oxidation wave was estimated to be 0.93 V by means of differential pulse voltammetry. FAM undergoes reversible oxidation at  $E_{1/2,ox} = 1.01 \text{ V}$ .

Compared to TMR and FAM, PTZ has a less-positive oxidation potential that can be correlated to the higher value of the highest occupied molecular orbital (HOMO) of the PTZ molecule compared to those of TMR and FAM. Therefore, when TMR or FAM is photochemically excited, an electron of PTZ can be easily transferred to the ground state of the excited TMR\* or FAM\*, thereby quenching its fluorescence emission (Figure 1 b). This observation provides an explanation to understand why PTZ can be used as a versatile quencher by the mechanism of PET for fluorophores including TMR and FAM. PTZ, which is a PET quencher, can be used to develop a more selective detection system than that developed by using Dab, which is a FRET quencher, because fluorescence quenching by electron transfer is

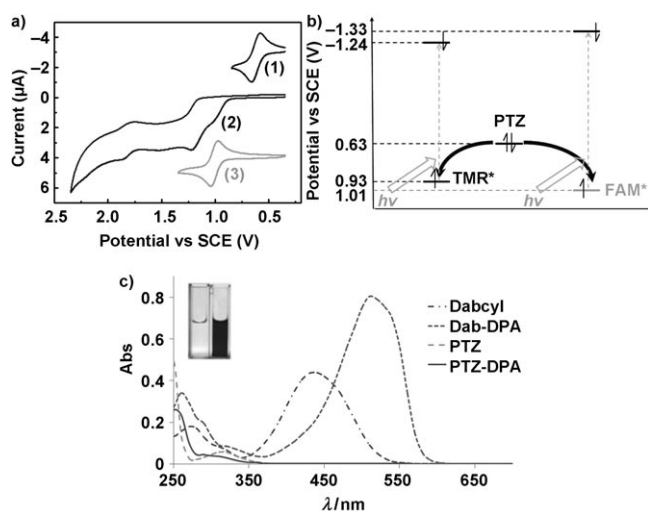


**Figure 1.** a) Cyclic voltammograms of 1) PTZ, 2) TMR, and 3) FAM, all 1 mM in acetonitrile (supporting electrolyte: 0.1 M TBAPF<sub>6</sub>), at a scan rate of  $200 \text{ mV s}^{-1}$ . b) Energy diagram of the quencher (PTZ) and fluorophores (TMR and FAM). The HOMO value corresponds to the oxidation potential. The LUMO values that correspond to the reduction potentials were estimated from the calculated emission energies of fluorophores ( $E_s = 1239.81/\lambda_{max} \text{ eV}$ ). c) UV/Vis absorption spectra of Dab-DPA (10  $\mu\text{M}$ ), Dab (10  $\mu\text{M}$ ), PTZ (10  $\mu\text{M}$ ), and PTZ-DPA (10  $\mu\text{M}$ ) in acetonitrile. Inset: PTZ-DPA (100  $\mu\text{M}$ , left) and Dab-DPA (100  $\mu\text{M}$ , right) in buffer solution. SCE = saturated calomel electrode.

efficient only at very short distances.<sup>[12]</sup> Furthermore, in the visible-light range, PTZ has a negligible molar extinction coefficient ( $\epsilon = 5740 \text{ cm}^{-1} \text{ M}^{-1}$ ,  $\lambda_{max} = 316 \text{ nm}$ ), whereas Dab has a high molar extinction coefficient ( $\epsilon = 44000 \text{ cm}^{-1} \text{ M}^{-1}$ ,  $\lambda_{max} = 436 \text{ nm}$ ); because of this high coefficient, inner filter effects<sup>[9a,b]</sup> become significant at high concentrations. In our experiment, Dab-DPA shows a far-red-shifted absorption band ( $\epsilon = 80600 \text{ cm}^{-1} \text{ M}^{-1}$ ,  $\lambda_{max} = 512 \text{ nm}$ ), but PTZ-DPA shows almost no absorption in the visible range. Therefore, PTZ is expected to be a more suitable fluorescence quencher for a selective quenching system.

We performed fluorescence titration experiments on Dab-DPA and PTZ-DPA by using ten fluorescent peptides (Table 1). FAM-abl showed nonspecific fluorescence quenching with both Dab-DPA and PTZ-DPA because the anionic fluorescein could bind to the bis( $Zn^{2+}$ -dipicolylamine) complex in Dab-DPA and PTZ-DPA, regardless of the peptide phosphorylation (see the Supporting Information). However, PTZ-DPA showed a higher fluorescence quenching ratio (0.72) than Dab-DPA (0.59) for nonphosphorylated and phosphorylated TMR-peptides (Figure 2a; see the Supporting Information). TMR-cas, which has a  $-7$  net charge, is expected to bind to PTZ-DPA more strongly than other nonphosphorylated peptides; however, TMR-p-cas showed a more distinct fluorescence quenching with PTZ-DPA than did TMR-cas, because PTZ-DPA bound strongly to TMR-p-cas rather than to TMR-cas (Figure 2b). Other nonphosphorylated and phosphorylated TMR-peptides were also clearly distinguished by PTZ-DPA (Figure 2b).

These results encouraged us to attempt real-time fluorescence monitoring of the activities of several kinases (PKA,

**Table 1:** Fluorescent peptides in kinase assay with PTZ-DPA.

Substrate	Target kinase	Sequence
FAM-abl	Abl kinase	FAM-KKGEAIYAAPFA-NH <sub>2</sub>
FAM-p-abl	–	FAM-KKGEAI-pY-AAPFA-NH <sub>2</sub>
TMR-abl	Abl kinase	TMR-KKGEAIYAAPFA-NH <sub>2</sub>
TMR-p-abl	–	TMR-KKGEAI-pY-AAPFA-NH <sub>2</sub>
TMR-pka	PKA <sup>[a]</sup>	TMR-LRRASLG-OH
TMR-p-pka	–	TMR-LRRA-pS-LG-OH
TMR-cam	CaMKII <sup>[b]</sup>	TMR-KKALRRQETVDAL-OH
TMR-p-cam	–	TMR-KKALRRQE-pT-VDAL-OH
TMR-cas	CKII <sup>[c]</sup>	TMR-RRADSDDDDD-OH
TMR-p-cas	–	TMR-RRADD-pS-DDDDD-OH

[a] Protein kinase A catalytic subunit. [b] Ca<sup>2+</sup>/calmodulin-dependent kinase II. [c] Casein kinase II. NH<sub>2</sub> and OH in the C terminal of peptides indicate amides and acids, respectively.

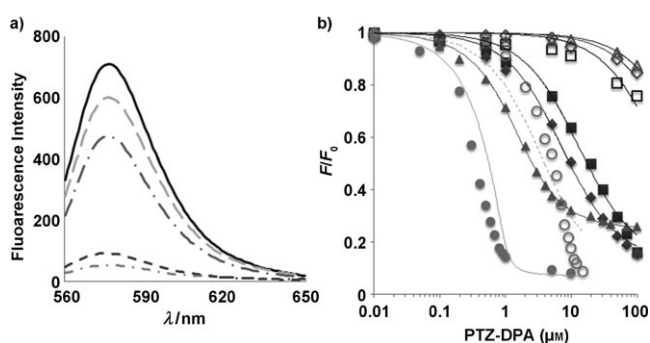


**Figure 2.** a) Fluorescence quenching of TMR-abl or TMR-p-abl upon the addition of PTZ-DPA or Dab-DPA in aqueous HEPES (10 mM, pH 7.4) buffer solution. TMR-abl, 1 μM (—); TMR-abl 1 μM+PTZ-DPA 100 μM (---); TMR-abl 1 μM+DabDPA 100 μM (- - -); TMR-p-abl 1 μM+PTZ-DPA 100 μM (- - -); TMR-p-abl 1 μM+DabDPA 100 μM (- - -). b) Fluorescence titration curves of peptides (1 μM each) upon the addition of PTZ-DPA (0.01–100 μM, 10 mM HEPES, pH 7.4). The x axis is a log scale. TMR-pka (□); TMR-p-pka (■); TMR-abl (◇); TMR-p-abl (◆); TMR-cam (△); TMR-p-cam (▲); TMR-cas (○); TMR-p-cas (●). HEPES = 4-(2-hydroxyethyl)-1-piperazineethanesulfonic acid.

Abl kinase, CaMKII, casein kinase II) by using PTZ-DPA. The fluorescence intensity of TMR-peptides (1 μM) in an enzymatic reaction mixture decreased rapidly with time upon the addition of PTZ-DPA (100 μM; Figure 3 and Figure S7 in

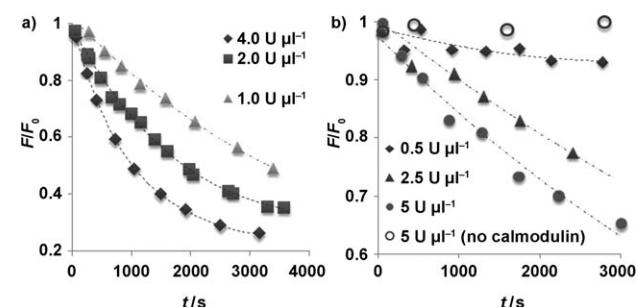


**Figure 3.** Real-time fluorescence monitoring of various kinase activities with PTZ-DPA using TMR-peptides. a) Abl protein kinase. b) Calmodulin-dependent kinase II (CaMKII).

the Supporting Information).<sup>[13]</sup> As expected, the peptide phosphorylation rate increased with the amount of kinase added to the reaction solutions. Furthermore, the calmodulin-dependent kinase II showed almost no activity when calmodulin was not added to the reaction solution (Figure 3 b).

We also performed control experiments in which fluorescent peptides (TMR-pka, TMR-cam) were incubated with Abl kinase. As expected, the fluorescence of TMR-pka and TMR-cam did not decrease upon the addition of PTZ-DPA (Figure S11A, Supporting Information); this was because these peptides could not be phosphorylated by Abl kinase. Furthermore, the fluorescence of TMR-abl incubated with PKA did not decrease but rather increased<sup>[14]</sup> upon the addition of PTZ-DPA, which might be caused by nonspecific interaction between fluorescent peptides and unsuitable kinases (see Figure S13 in the Supporting Information). Therefore, we concluded that the fluorescence of fluorescent peptides decreases upon treatment with PTZ-DPA only when they are phosphorylated by suitable kinases. This orthogonality between peptide substrates and kinases can be very useful for an in vitro assay of target kinases in cellular lysates.

Note that both Dab-DPA and PTZ-DPA also bind to ATP and adenosine 5'-diphosphate (ADP), which are the substrate and by-product, respectively, of the protein kinase reaction. This can interfere with monitoring of peptide phosphorylation by Dab-DPA and PTZ-DPA. Nevertheless, the problem can be solved if a higher concentration of the quencher probe (100 μM) than those of ATP (2 μM) and the fluorescent peptides (1 μM) is used for the estimation of peptide phosphorylation.

We also carried out fluorescent screening of kinase inhibitors such as Gleevec (imatinib mesylate, Abl kinase inhibitor)<sup>[15a]</sup> and A3-hydrochloride (PKA inhibitor).<sup>[15b]</sup> As shown in Figure S11B in the Supporting Information, we found that the reaction rate decreased upon the addition of each inhibitor to the corresponding enzymatic reaction mixture. As shown in our experimental data, we obtained the IC<sub>50</sub> value (820 nM; Figure S12, Supporting Information) of Gleevec, which is comparable to that obtained in other studies.<sup>[16]</sup> These results show the potential for the utilization of quencher probes in high-throughput screening for drug development.

The quencher probes PTZ-DPA and TMR-abl were also used for the diagnosis of CML.<sup>[17]</sup> It is well known that aberrant Abl kinase activity (Bcr-Abl)<sup>[17a,b]</sup> is one of the major factors that cause myeloid leukemia. At present, most of the CML diagnosis methods, such as cytogenetic analysis<sup>[17c]</sup> or polymerase chain reaction analysis for the Bcr-Abl gene,<sup>[17c]</sup> are performed at the genomic level. However, detecting Abl kinase activity directly from patients' bone marrow samples is also crucial. We performed blind tests by using four bone marrow samples from CML patients and from a healthy person.<sup>[18]</sup>

As shown in Figure 4 a, we achieved distinctive real-time fluorescence monitoring of Abl kinase activity in the sample lysates by using PTZ-DPA. From the obtained data, we could clearly discriminate the sample of a patient from that of a healthy subject; the rates of phosphorylation of TMR-abl in the case of CML patients were higher than those in the case of

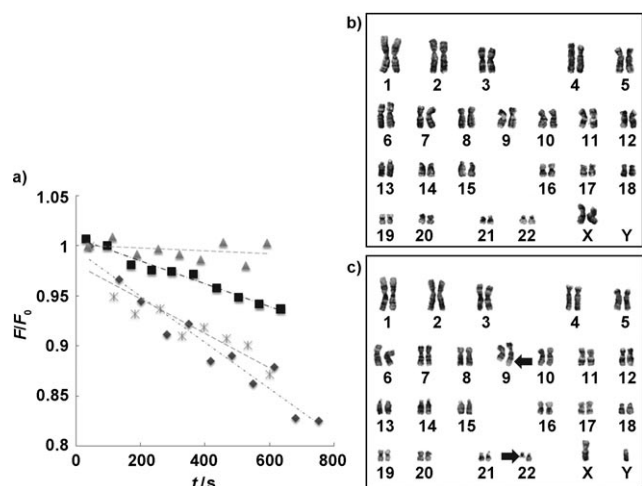


**Figure 4.** a) Fluorescence detection of phosphorylation of TMR-abl in CML patient samples by using PTZ-DPA. CML, chronic phase ( $\blacklozenge$ ); control (person;  $\blacksquare$ ); CML, chronic phase, resistant to drugs ( $\triangle$ ); CML, complete hematological response ( $\triangle$ ). b) Karyotype of a control sample (healthy person). c) Karyotype of a CML (chronic phase) sample.

a healthy person. Furthermore, negligible Abl kinase activity was observed in the sample of a person with a complete hematologic response to CML. We also performed a conventional cytogenetic study (Figure 4b and c; see the Supporting Information) to check for the presence of Philadelphia chromosomes<sup>[18b]</sup> in the samples that were determined by our sensing system to belong to the healthy person (Figure 4b) or to CML patients (chronic phase, Figure 4c). To the best of our knowledge, this is the first use of synthetic probes for cancer diagnosis. Our results show that PTZ-DPA and

other fluorescent peptide substrates can be powerful tools for cancer diagnosis.

Because our kinase activity detection method using PTZ-DPA is based on fluorescence intensity (ON/OFF), we believe that a kinase assay system can be built on microfluidic chips, in which only a few nanoliters of a solution are required for detection.<sup>[19]</sup> In these microfluidic chips (Figure 5a and b), an enzymatic reaction mixture is incubated for 1 h, diluted (20  $\mu\text{M}$  TMR-peptide, 40  $\mu\text{M}$  ATP, with or without kinase and kinase reaction buffer), and allowed to flow through the upper half of the mixing circle; the PTZ-DPA solution (200  $\mu\text{M}$ , pH 7.4, 10 mM HEPES) flowed through the lower half. The two parts were mixed sequentially for 1 min with the help of electronically controlled  $\text{N}_2$ -gas valves for 1 min. Then, the fluorescence of the mixture was measured under a fluorescence stereo microscope (see the Supporting Information). As expected, the fluorescence of each TMR-peptide was quenched by PTZ-DPA only when the peptide was phosphorylated with PKA (Figure 5c and d), Abl kinase (Figure 5e and f), or CaMKII (Figure 5g and h). We also monitored the dephosphorylation of TMR-p-pka by alkaline phosphatase (ALP) in the microfluidic chips (Figure 5i and j). To the best of our knowledge, this is the first report of a homogeneous kinase assay involving the use of microfluidic chips.

In conclusion, we have demonstrated a novel fluorescent kinase assay based on the use of selective fluorescence quencher probes (Dab-DPA, PTZ-DPA) for phosphorylated fluorescent peptides. With this probe, we can perform kinase inhibitor tests and diagnose CML on the basis of the detection of Abl kinase activity in the patients' myelogenous samples. We also developed the first homogeneous fluorescent kinase assay system on microfluidic chips. This detection system involves the use of a quencher probe and has the potential to be applied to the development of kinase inhibitors by high-

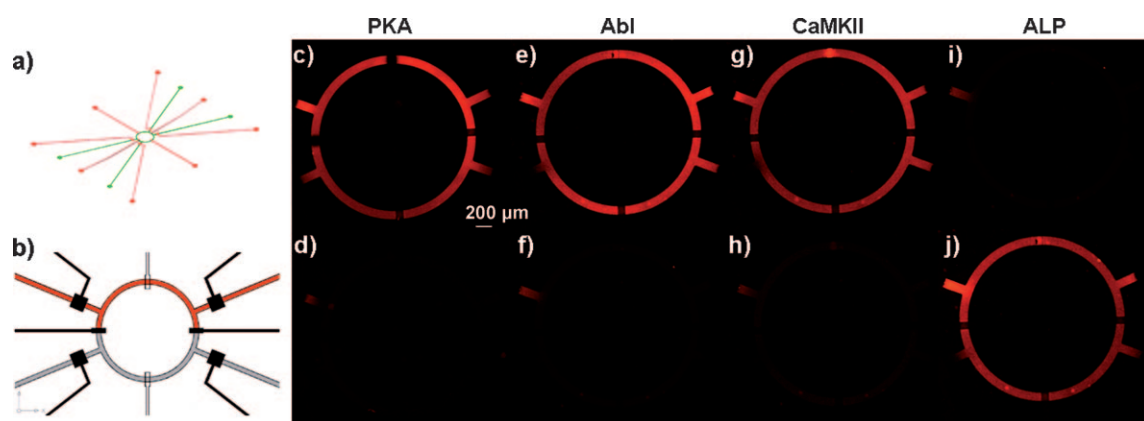


**Figure 5.** Kinase assay on a microfluidic chip: a) microfluidic chip design; b) microfluidic mixing circle: kinase reaction mixture pathway (red, upper half circle), PTZ-DPA solution pathway (gray, lower half circle), closed valve (black), opened valve (white); c) 10  $\mu\text{M}$  TMR-pka, 20  $\mu\text{M}$  ATP, no PKA, 100  $\mu\text{M}$  PTZ-DPA; d) 10  $\mu\text{M}$  TMR-pka, 20  $\mu\text{M}$  ATP, 12.0  $\text{U}\mu\text{L}^{-1}$  PKA, 100  $\mu\text{M}$  PTZ-DPA, 10 mM  $\text{MgCl}_2$ , reaction buffer of (c,d): 10 mM  $\text{MgCl}_2$ , pH 7.5, 50 mM Tris-HCl; e) 10  $\mu\text{M}$  TMR-abl, 20  $\mu\text{M}$  ATP, no Abl kinase, 100  $\mu\text{M}$  PTZ-DPA; f) 10  $\mu\text{M}$  TMR-abl, 20  $\mu\text{M}$  ATP, 10  $\text{U}\mu\text{L}^{-1}$  Abl kinase, 100  $\mu\text{M}$  PTZ-DPA, reaction buffer of (e,f): 50 mM Tris-HCl, 10 mM  $\text{MgCl}_2$ , 2 mM DTT, 1 mM EGTA, 0.01% Brij 35; g) 10  $\mu\text{M}$  TMR-cam, 20  $\mu\text{M}$  ATP, no CaMKII, 100  $\mu\text{M}$  PTZ-DPA; h) 10  $\mu\text{M}$  TMR-cam, 20  $\mu\text{M}$  ATP, 5.0  $\text{U}\mu\text{L}^{-1}$  CaMKII, 100  $\mu\text{M}$  PTZ-DPA, reaction buffer of (g,h): 50 mM Tris-HCl, 10 mM  $\text{MgCl}_2$ , 2 mM DTT, 0.1 mM  $\text{Na}_2\text{EDTA}$ , 1.2  $\mu\text{M}$  calmodulin, 2 mM  $\text{CaCl}_2$ ; i) 10  $\mu\text{M}$  TMR-p-pka, 100  $\mu\text{M}$  PTZ-DPA, no ALP; j) 10  $\mu\text{M}$  TMR-p-pka, 2.5  $\mu\text{g}\mu\text{L}^{-1}$  ALP, 100  $\mu\text{M}$  PTZ-DPA, reaction buffer of (i,j): 10 mM  $\text{MgCl}_2$ , pH 7.5, 50 mM Tris-HCl. DTT = dithiothreitol, EGTA = ethylene glycol tetraacetic acid, EDTA = ethylenediamine tetraacetic acid.

throughput screening and for the diagnosis of diseases caused by irregular kinase activities.

Received: February 12, 2010

Revised: April 14, 2010

Published online: June 10, 2010

**Keywords:** cancer · fluorescence · fluorescent probes · kinases · phosphorylation

- [1] a) G. Manning, D. B. Whyte, R. Martinez, T. Hunter, S. Sudarsanam, *Science* **2002**, *298*, 1912; b) P. Blume-Jensen, T. Hunter, *Nature* **2001**, *411*, 355.
- [2] a) H. Zhu, J. F. Klemic, S. Chang, P. Bertone, A. Casamayor, K. G. Klemic, D. Smith, M. Gerstein, M. A. Reed, M. Snyder, *Nat. Genet.* **2000**, *26*, 283; b) M.-L. Lesaichere, M. Uttamchandani, G. Y. J. Chen, S. Q. Yao, *Bioorg. Med. Chem. Lett.* **2002**, *12*, 2085; c) H. Zhu, M. Snyder, *Curr. Opin. Chem. Biol.* **2003**, *7*, 55; d) Y.-P. Kim, Y.-H. Oh, H.-S. Kim, *Biosens. Bioelectron.* **2008**, *23*, 980.
- [3] a) M. Sills, D. Weiss, Q. Pham, R. Schweitzer, X. Wu, J. Wu, *J. Biomol. Screening* **2002**, *7*, 191; b) R. Seethala, R. Menzel, *Anal. Biochem.* **1997**, *253*, 210; c) E. R. Sharlow, S. Leimgruber, A. Yellow-Duke, R. Barrett, Q. J. Wang, J. S. Lazo, *Nat. Protoc.* **2008**, *3*, 1350; d) J. Beasley, D. Dunn, T. Walker, S. Parlato, J. Lehrach, D. Auld, *Assay Drug Dev. Technol.* **2003**, *1*, 455.
- [4] a) R. H. Yeh, X. Yan, M. Cammer, A. R. Bresnick, D. S. Lawrence, *J. Biol. Chem.* **2002**, *277*, 11527; b) C.-A. Chen, R.-H. Yeh, D. S. Lawrence, *J. Am. Chem. Soc.* **2002**, *124*, 3840; c) W. F. Veldhuyzen, Q. Nguyen, G. McMaster, D. S. Lawrence, *J. Am. Chem. Soc.* **2003**, *125*, 13358; d) Q. Wang, D. S. Lawrence, *J. Am. Chem. Soc.* **2005**, *127*, 7684; e) Q. Wang, S. M. Cahill, M. Blumenstein, D. S. Lawrence, *J. Am. Chem. Soc.* **2006**, *128*, 1808; f) Z. Dai, N. G. Dulyaninova, S. Kumar, A. R. Bresnick, D. S. Lawrence, *Chem. Biol.* **2007**, *14*, 1254; g) D. S. Lawrence, Q. Wang, *ChemBioChem* **2007**, *8*, 373; h) V. Sharma, R. S. Agnes, D. S. Lawrence, *J. Am. Chem. Soc.* **2007**, *129*, 2742; i) V. Sharma, Q. Wang, D. S. Lawrence, *Biochim. Biophys. Acta Proteomics Proteomics* **2008**, *1784*, 94; j) A. Wakata, S. M. Cahill, M. Blumenstein, R. H. Gunby, S. Jockusch, A. A. Marti, B. Cimbri, C. Gambacorti-Passerini, A. Donella-Deana, L. A. Pinna, N. J. Turro, D. S. Lawrence, *Org. Lett.* **2008**, *10*, 301.
- [5] a) M. D. Shults, B. Imperiali, *J. Am. Chem. Soc.* **2003**, *125*, 14248; b) D. M. Rothman, M. D. Shults, B. Imperiali, *Trends Cell Biol.* **2005**, *15*, 502; c) M. D. Shults, K. A. Janes, D. A. Lauffenburger, B. Imperiali, *Nat. Methods* **2005**, *2*, 277; d) M. D. Shults, D. Carrico-Moniz, B. Imperiali, *Anal. Biochem.* **2006**, *352*, 198; e) B. R. Sculimbrene, B. Imperiali, *J. Am. Chem. Soc.* **2006**, *128*, 7346; f) E. Luković, J. A. Gonzalez-Vera, B. Imperiali, *J. Am. Chem. Soc.* **2008**, *130*, 12821; g) J. A. González-Vera, E. Luković, B. Imperiali, *Bioorg. Med. Chem. Lett.* **2009**, *19*, 1258; h) E. Luković, E. Vogel Taylor, B. Imperiali, *Angew. Chem.* **2009**, *121*, 6960; *Angew. Chem. Int. Ed.* **2009**, *48*, 6828.
- [6] a) M. S. Tremblay, Q. Zhu, A. A. Marti, J. Dyer, M. Halim, S. Jockusch, N. J. Turro, D. Sames, *Org. Lett.* **2006**, *8*, 2723; b) M. S. Tremblay, M. Lee, D. Sames, *Org. Lett.* **2008**, *10*, 5.
- [7] T. Anai, E. Nakata, Y. Koshi, A. Ojida, I. Hamachi, *J. Am. Chem. Soc.* **2007**, *129*, 6232.
- [8] a) A. Y. Ting, K. H. Kain, R. L. Klemke, R. Y. Tsien, *Proc. Natl. Acad. Sci. USA* **2001**, *98*, 15003; b) J. Zhang, Y. Ma, S. S. Taylor, R. Y. Tsien, *Proc. Natl. Acad. Sci. USA* **2001**, *98*, 14997.
- [9] a) E. D. Matayoshi, G. T. Wang, G. A. Krafft, J. Erickson, *Science* **1990**, *247*, 954; b) Y. Liu, W. Kati, C.-M. Chen, R. Tripathi, A. Molla, W. Kohlbrenner, *Anal. Biochem.* **1999**, *267*, 331; c) J. Li, X. Fang, W. Tan, *Biochem. Biophys. Res. Commun.* **2002**, *292*, 31.
- [10] B. König, M. Pelka, H. Zieg, T. Ritter, H. Bouas-Laurent, R. Bonneau, J. Desvergne, *J. Am. Chem. Soc.* **1999**, *121*, 1681.
- [11] a) A. Ojida, I. Takashima, T. Kohira, H. Nonaka, I. Hamachi, *J. Am. Chem. Soc.* **2008**, *130*, 12095; b) A. Ojida, H. Nonaka, Y. Miyahara, S. Tamaru, K. Sada, I. Hamachi, *Angew. Chem.* **2006**, *118*, 5644; *Angew. Chem. Int. Ed.* **2006**, *45*, 5518; c) W. M. Leevy, S. T. Gammon, H. Jiang, J. R. Johnson, D. J. Maxwell, E. N. Jackson, M. Marquez, D. Piwnica-Worms, B. D. Smith, *J. Am. Chem. Soc.* **2006**, *128*, 16476; d) H. Jiang, E. J. O'Neil, K. M. Divittorio, B. D. Smith, *Org. Lett.* **2005**, *7*, 3013; e) H.-W. Rhee, H. Y. Choi, K. Han, J.-I. Hong, *J. Am. Chem. Soc.* **2007**, *129*, 4524; f) H.-W. Rhee, C. R. Lee, S. H. Cho, M. R. Song, M. Cashel, H. E. Choy, Y. J. Seok, J.-I. Hong, *J. Am. Chem. Soc.* **2008**, *130*, 784; g) H.-W. Rhee, S. J. Choi, S. H. Yoo, Y. O. Jang, H. H. Park, P. M. Pinto, J. C. Cameselle, F. J. Sandoval, S. Roje, K. Han, D. S. Chung, J. Suh, J.-I. Hong, *J. Am. Chem. Soc.* **2009**, *131*, 10107.
- [12] J. R. Lakowicz, *Principles of Fluorescence Spectroscopy*, Springer, New York, **2006**.
- [13] The phosphorylation of TMR-abl by Abl kinase was also confirmed by HPLC monitoring (see the Supporting Information).
- [14] A. Yamagata, R. Masui, R. Kato, N. Nakagawa, H. Ozaki, H. Sawai, S. Kuramitsu, K. Fukuyama, *J. Biol. Chem.* **2000**, *275*, 13235.
- [15] a) B. Druker, S. Tamura, E. Buchdunger, S. Ohno, G. Segal, S. Fanning, J. Zimmermann, N. Lydon, *Nat. Med.* **1996**, *2*, 561; b) M. Inagaki, S. Kawamoto, H. Itoh, M. Saitoh, M. Hagiwara, J. Takahashi, H. Hidaka, *Mol. Pharm.* **1986**, *29*, 577.
- [16] a) C. S. Lebakken, S. M. Riddle, U. Singh, W. J. Frazee, H. C. Eliason, Y. Gao, L. J. Reichling, B. D. Marks, K. W. Vogel, *J. Biomol. Screening* **2009**, *14*, 924; b) J.-L. Tardieu, T. Roux, *BIOforum Eur.* **2007**, *6*, 42.
- [17] a) S. Faderl, M. Talpaz, Z. Estrov, S. O'Brien, R. Kurzrock, H. Kantarjian, *N. Engl. J. Med.* **1999**, *341*, 164; b) R. Kurzrock, H. M. Kantarjian, B. J. Druker, M. Talpaz, *Ann. Intern. Med.* **2003**, *138*, 819; c) F. Mitelman, *Leuk. Lymphoma* **1993**, *11*, 11; d) T. Hughes, S. Branford, *Blood Rev.* **2006**, *20*, 29.
- [18] a) These samples were also confirmed by cytogenetic analysis; b) Philadelphia chromosome is an abnormal chromosomal translocation caused by the juxtapositioning of part of the *BCR* gene from chromosome 22 (region q11) to the *Abli* gene on chromosome 9 (region q34). 95% of the people with CML have this reciprocal translocation between chromosomes 9 and 22. See Ref. [16].
- [19] S. Kou, H. N. Lee, D. van Noort, K. M. Swamy, S. H. Kim, J. H. Soh, K. M. Lee, S. W. Nam, J. Yoon, S. Park, *Angew. Chem.* **2008**, *120*, 886; *Angew. Chem. Int. Ed.* **2008**, *47*, 872.